Defect induced structural transitions, instability and plastic strain localization in dynamically loaded metals

Mikhail Sokovikov[a] , Vasiliy Chudinov,
Sergey Uvarov, Oleg Plekhov, Elena Lyapunova, Oleg Naimark[b]

Institute of Continuous Media Mechanics of Ural Branch of Russian Academy of Sciences
1 Ak. Korolev Street, 614013 Perm, Russia

[a]sokovikov@icmm.ru, [b]naimark@icmm.ru

Keywords: instability and localization of plastic strain; high-velocity perforation; non-equilibrium transitions; micro-shears.

Abstract. We present an experimental and theoretical study of the mechanisms of plastic strain instability in metals subjected to dynamic loading. A special sample shape was proposed to realize pure shear strain localization state using Hopkinson-Kolsky bar apparatus. The lateral strain localization area was studied in-situ using a high-speed infra-red camera CEDIP Silver 450M with sensitivity ~25 mK (at 300K), spectral range 3-5 mkm, maximum frame size 320x240 pixels and temporal resolution 1KHz. The temperature field distribution obtained at different time allowed us to trace the evolution of plastic strain localization and support theoretical results concerning the leading role of defect-induced structural transitions in the mechanisms of plastic strain localization.

Intrudiction

In this study, we consider the instability and localization of plastic deformation in metals during the high-speed perforation process. Theoretical studies have been carried out using the previously developed theory, in which the methods of statistical physics and thermodynamics of irreversible processes are applied to explore the influence of microshears on the plastic properties of solids [1-3].

These results were applied to the experimental study of perforation of a target due to the plug formation. The plug ejection at impact velocities of 101 – 260 м/с was studied using high-speed infrared scanning and VISAR technique to measure the plug velocity kinetics. The original ballistic set-up for studying perforation was used to test A6061 alloy samples in different pulse loading regimes followed by plastic flow instability and plug ejection.

Changes in the velocity of a rear surface at different time of plug ejection were analyzed by means of VISAR data. The microstructure analysis of recovered samples was performed using the New View interferometer-profilometer and a scanning electron microscope. Processing of 3D data obtained for the defect-induced deformation relief at different time of the plug ejection provided the estimation of plastic strain gradient distribution.

It is shown that the strain distribution is relatively uniform in the initial penetration stage with a smooth mirror-like fracture surface, whereas in the plug formation and the ejection regions it becomes essentially non-uniform along the radius of a normal to the sample surface. Localization of plastic strain occurs in a thin region providing the plug formation. As the plug moves, the surface relief undergoes the roughening effect, and the local inhomogeneities of shear deformation become larger. The development of plastic shear instability regions is simulated numerically. For this purpose, a recently developed theory is used, in which the influence of the collective behavior of microshears on the strain localization has been described using the statistically based thermodynamics of a solid with mesodefects.

Experimental study

An abrupt transition to a more ordered defect structure often leads to anomalies in deformation properties, which may occur, particularly, in the case of high-speed collisions of a projectile with a target[4-7].

Al-6061 alloy specimens were loaded using a perforation testing machine (Fig.1, 2). This setup is assembled on frame (7) and consists of high-pressure chamber (1), barrel (2), photosensor (3), target (9), target fixing device (8) with stopping mechanism (6), receiving chamber (10), and trapping device (11).

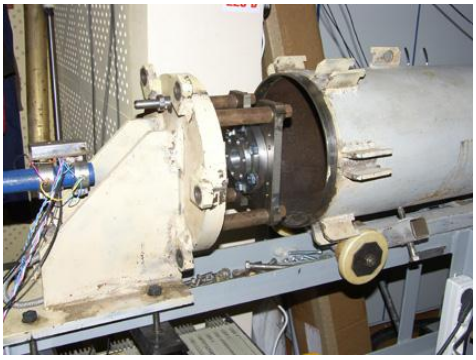

Fig.1.Testing machine for specimen perforation.

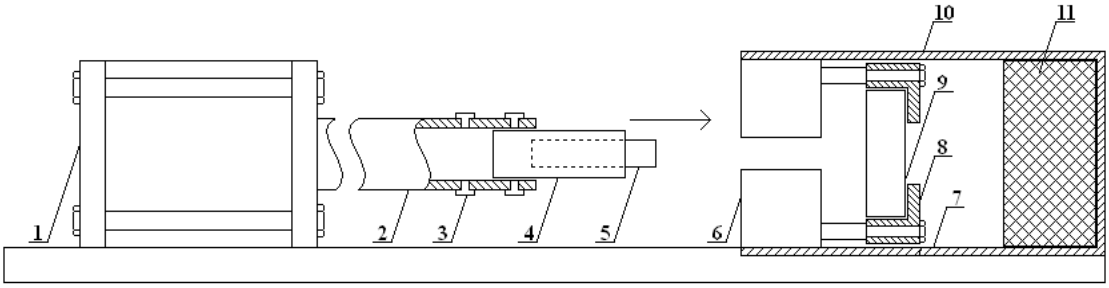

Fig.2. Schematic diagram of the perforation testing machine.1 – high-pressure chamber, 2 – barrel, 3 – photosensor, 4 – chuck, 5 – projectile, 6 – stopping mechanism, 7 – frame, 8 – target fixing device, 9 – target, 10 – receiving chamber, 11 – trapping device.

To accelerate the projectile in the barrel, an ebonite chuck (Fig.3a) with an external diameter corresponding to the size of the barrel bore is used. The barrel has special grooves that create an air gap for reducing friction between the plate and the barrel. A high-carbon steel rod of 5 mm diameter, 50 mm long and of weight of 7.4 g is used as a projectile.

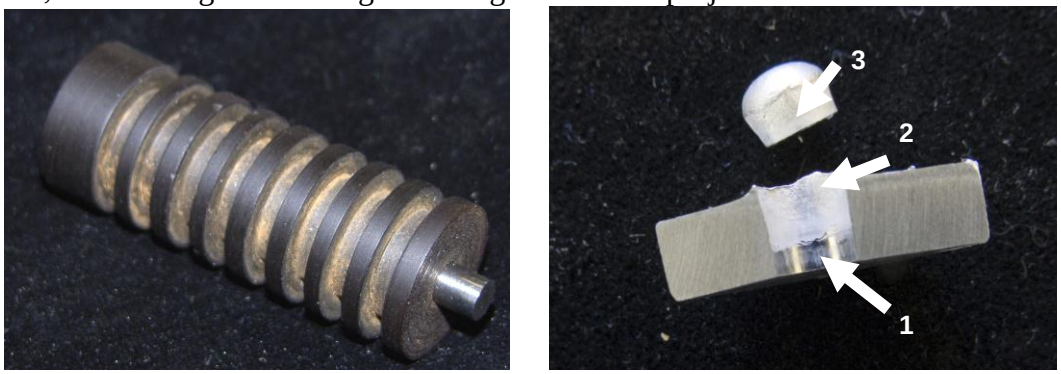

a b

Fig.3.a) projectile enclosed in the chuck.

b) The structure of failure surfaces of the specimen and plug: 1 - mirror image; 2- rough surfaces; 3 - the plug.

The velocity of the chuck with the projectile is determined by measuring the transit time between the two photosensors. In front of the target, there is a stopping mechanism with an inner diameter smaller than the outer diameter of the chuck, but greater than the diameter of the projectile. While colliding with the stopping mechanism, the chuck slows down and then gets destroyed, and the projectile continues to move up to the collision with the target. In the event of high-speed projectile-target interaction, the failure is realized as plug formation and ejection. Figure 3b shows the specimen cut across the diameter and the ejected plug. The projectile and plug that continue to move after target perforation are captured in the receiving chamber by soft filler, which makes it possible to avoid the distortion of the plug shape.

To study the distribution of plastic deformations in the process of plug formation and ejection, a high-speed infrared camera CEDIP Silver 450M was employed. The experimental setup is shown in Fig. 4.

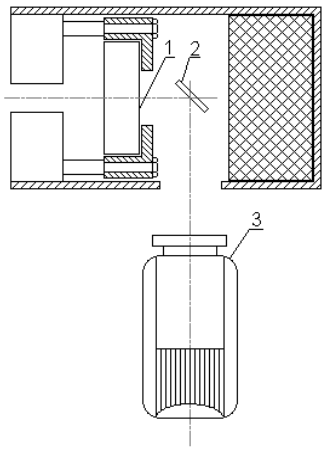

Fig.4.Scheme of the target perforation experiment performed with a high-speed infrared camera. 1 – specimen, 2 – mirror, 3 – infrared camera

Fig.5 shows the infrared images of the plugged hole and the flying pug. The velocity, at which the projectile strikes the target, is 120m/s.The maximum temperature at the hole periphery is 62^0C.

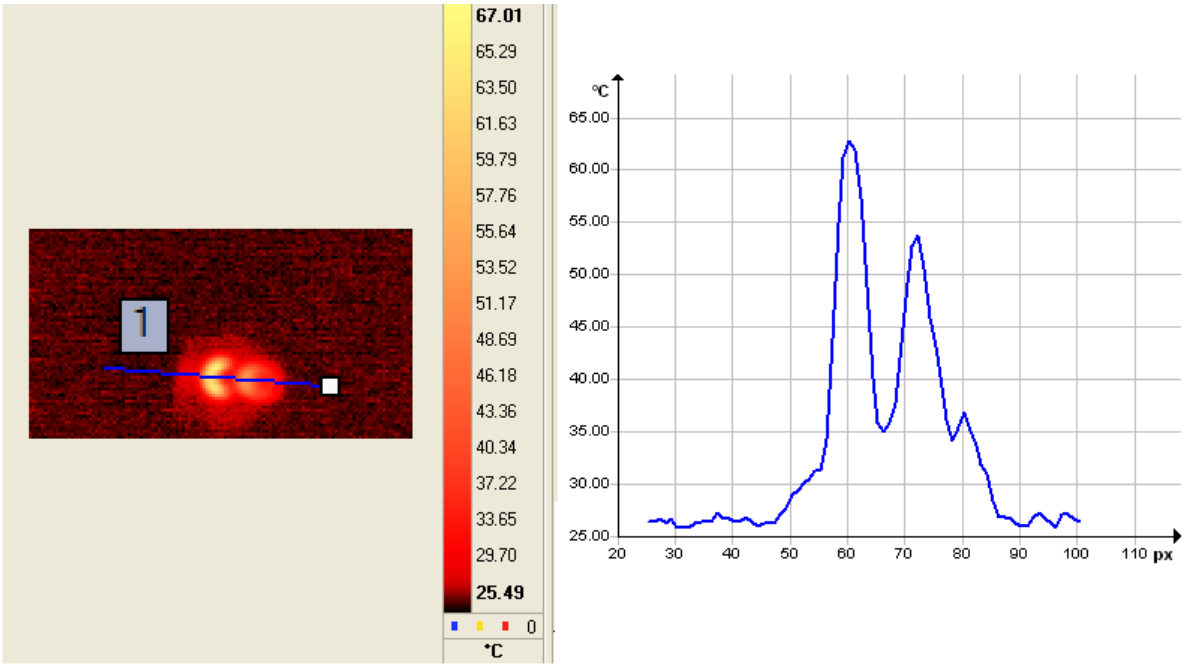

Fig.5. Infrared images of the plugged hole and the flying plug

Fig.6 presents an infrared picture illustrating the back surface of the target in the process of plug formation.

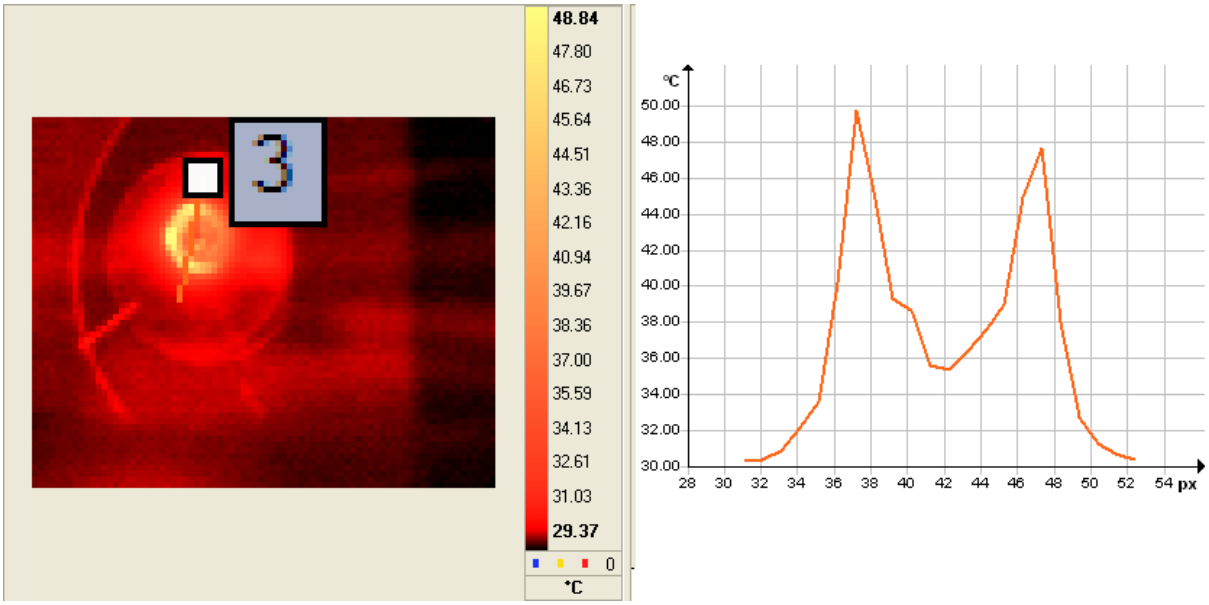

Fig.6. Infrared images of plugging. The maximum temperature at the periphery of the hole is 49^0C.

Application of the infrared camera for real-time observation of the target response during the perforation tests has shown that the temperature values in the areas of localization of plastic deformation do not exceed ~ 100^0C, which is indicative of the feasibility of the mechanisms of plug formation and ejection unrelated to thermoplastic instability.
The process of plug formation and ejection was studied using a laser Doppler velocimeter VISAR. As a result, we obtained the time dependence of the free surface velocity in the area of plug formation and ejection.

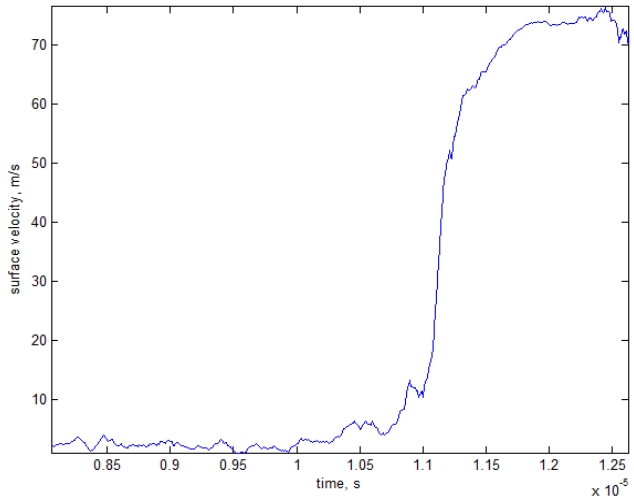

Fig.8. Time dependence of the free surface velocity in the area of plug formation and ejection.

After the completion of the test, the microstructure of the deformed specimens was analyzed with the aid of an optical microscope-interferometer NewView-5000 and a scanning electron microscope.

It has been found that the distribution of strain is relatively uniform in the initial penetration region with a smooth mirror-like fracture surface, whereas in the plug formation and ejection regions it becomes essentially non-uniform over the radius of the specimen. The localization of plastic strain occurs in a thin region on the plug generation.
As the plug moves, the relief of the fracture surface becomes rougher, and the local heterogeneities of shear deformations increase due to distortion of the internal structure of the material.
In this case, one can observe the iron pieces of the projectile and grooves occurred due to friction between the rough-polished end-part of the projectile and the material.
The analysis of the rough surface with the scanning electron microscope has revealed the existence of two regions of different morphology: homogeneous in the middle part of the specimen and rougher near its back surface (Fig.9).The relatively homogeneous rough surface next to the mirror surface corresponds to the shear mechanism of deformation of the material and subsequent coarsening of the deformation structures (Fig.9b).

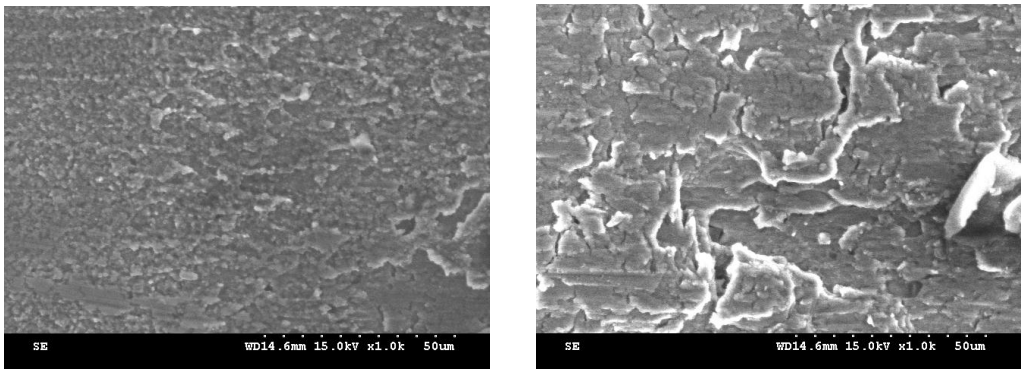

a) b)

Fig.9. Rough surface relief corresponding to the plug shear in the specimen. a) rough region near the mirror region, b) rough region at a distance from the mirror region.

The results of microstructural studies have indicated a significant role of multi-scale instability processes taking place in the microshear ensembles in the localization of plastic strain.

Modeling

In this paper, the mechanisms of plastic shear instability and localization of plastic deformation (in the quasi-one-dimensional statement) have been simulated numerically, and the peculiarities of the kinetics of microshear accumulation in the material have been analyzed.
We consider the deformation of a plane layer under pure shear loading. One side of the layer is rigidly fixed, and the other side is moving with a constant velocity v_0 (Fig.10).

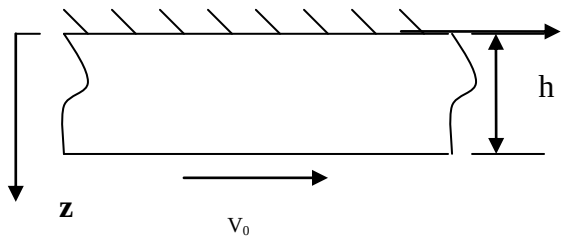

Fig.10. Scheme of loading

Taking into account the kinetics off microshear accumulation in the material, the behavior of the plane layer is described by the following equations:

$$\frac{\rho_0}{V}\frac{\partial v_x}{\partial t}=\frac{\partial \tau_{xz}}{\partial z}, \tag{1}$$

$$\tau_{xz}=l_1\dot{\varepsilon}^p_{xz}-l_2\frac{\partial p}{\partial t}, \tag{2}$$

$$\frac{\partial p}{\partial t}=\frac{l_2}{l_3}\dot{\varepsilon}^p_{xz}-\frac{1}{l_3}\Pi, \tag{3}$$

$$\Pi=-A_1\tau_{xz}\exp(-p_a/p)+B_1(p-p_b)-D_1\frac{\partial}{\partial z}\left(p\frac{\partial p}{\partial z}\right), \tag{4}$$

where l_1, l_2, l_3 are the kinetic coefficients, A_1, B_1, p_a, p_b are the approximation parameters, and p_z is the component of the microshear density tensor.

The initial and boundary conditions are written as

$$\tau_{xz}(z,0)=0;\ v_x(0,t)=0;\ v_x(h,t)=v_0, \tag{5}$$

$$p(z,0)=p_0\sin^8(\pi z);\ \frac{\partial p}{\partial z}(0,t)=\frac{\partial p}{\partial z}(h,t)=0. \tag{6}$$

The inhomogeneous plastic flow of the layer material and further localization of plastic deformation are activated by the initial non-uniform distribution of the microshear density tensor.

The elastic and plastic rates of strain are assumed to be additive. Thus we can write

$$\dot{\varepsilon}_{xz}=\dot{\varepsilon}^e_{xz}+\dot{\varepsilon}^p_{xz}. \tag{7}$$

The behavior of the layer of the material is described by the equation

$$\frac{\partial \tau_{xz}}{\partial t}=G\left(\frac{\partial v_x}{\partial z}-\dot{\varepsilon}^p_{xz}\right), \tag{8}$$

where G is the shear modulus.

During the process of high-speed deformation of the material, a structurally kinetic density transition in the microshear ensemble occurs in the local area. This transition is characterized by the jump in the microshear density parameter (Fig.11), which leads to a sharp abrupt change in the effective characteristics of the material, in particular, to a sharp decrease in the effective viscosity, and, as a consequence, to an increase in the plastic deformation and stress relaxation rates and to a decrease in the shear resistance in this area (Fig.11b).

The proposed model of the elasto-plastic behavior of the material takes into account the kinetics of microshear accumulation and describes the processes of plastic shear instability and plastic strain localization.

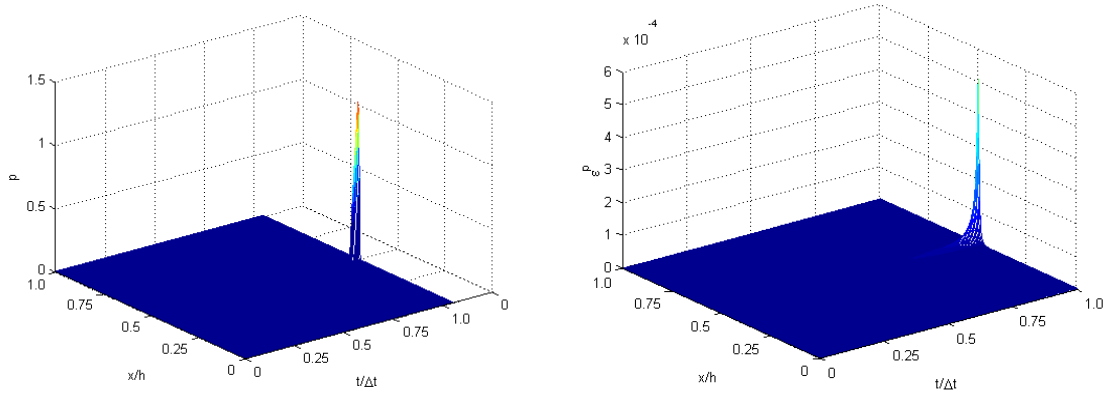

a b

Fig.11. Microshear density (a) and plastic strain rate(b) versus the coordinate and time.

Discussion of results

Based on the temperature measurements of the specimen surface at the time of plug formation and ejection and using the data obtained in the microstructural studies and numerical simulations, we can suggest that one of the mechanisms of plastic shear instability and plastic strain localization observed in the high-speed perforation tests is caused by structural- kinetic transitions in microshear ensembles.

This work was supported by grants within the research programs of the Presidium of RAS 09-П-1-1011 and by the RFBR grant (09-01-920005-HHC_a, 11-01-00712_a).

References

[1] Naimark, O.B. Kinetic transition in ensembles of microcracks and some nonlinear aspects of fracture. In: Proceedings IUTAM Symposium on nonlinear analysis of fracture. Kluver, The Netherlands, 1996.

[2] Naimark, O.B. Collective properties of mesodefect ensembles and some nonlinear plasticity and failure problems // Physical Mesomechanics, 2004, V.6, P. 45-72.

[3] Naimark, O.B. Structural-scaling transitions in solids with defects and some symmetric aspects of the field theory. Physical Mesomechanics, Tomsk. 2010. - V. 13. - No 5. - P. 113-126

[4] Jonas G.H. and Zukas J.A. Mechanics of penetration: analysis and experiments// Int. J. Eng. Sci. – 1978. – N11. – P.879-900.

[5] Sokovikov, M.A. Numerical study of plastic shear instability under dynamic loading.// Mathematical modeling of systems and processes. Collected papers No12, Perm, 2004, P. 82-88.

[6] Sokovikov, M.A. Self-similarity of plastic shear instability under impact loading as a result of kinetic transitions in the microshear ensemble. Physical Mesomechanics, V.7, special issue P.1, 2004, P.332-335.

[7] Sokovikov, M.A. Numerical study of oplastic shear instability under high-speed impact loading //Deformation and Fracture of Materials N7, 2005, P.13-17.